PHYSICAL REVIEW A **76**, 035401 (2007)

Effects of orientation and alignment in high-order harmonic generation and above-threshold ionization

C. B. Madsen, A. S. Mouritzen, T. K. Kjeldsen, and L. B. Madsen
Lundbeck Foundation Theoretical Center for Quantum System Research, Department of Physics and Astronomy, University of Aarhus, 8000 Aarhus C, Denmark

(Received 26 March 2007; published 24 September 2007)

When molecules interact with light sources of femtosecond or shorter duration the rotational degrees of freedom are frozen during the response to the strong nonperturbative interaction. We analytically derive how the frozen degrees of freedom affect the measurable signals in high-order harmonic generation and above-threshold ionization. High-order harmonic generation exhibits optical coherence in the signal from different orientations of the molecule. For ionization, the contributions from different orientations are added incoherently. The consequences of these findings are illustrated by numerical results.

DOI: 10.1103/PhysRevA.76.035401 PACS number(s): 33.80.Rv, 42.65.Ky

Currently, intense femtosecond pulses are produced in several laser laboratories worldwide. It is of fundamental interest to investigate how such pulses interact with quantum systems. As this research field is maturing [1], interesting applications are evolving: tomographic reconstruction [2], laser-induced electron diffraction [3], and molecular clocks [4–7] being examples under current study. Molecules are particularly well suited for such studies since they inherently carry the time scales that match those of the new laser sources: nuclei move on the femtosecond time scale, electrons on the attosecond time scale. Hence, the new light sources are perfect for looking inside molecules and for gaining insight into nuclear and electronic dynamics. Conversely, if the dynamics of the system under study is well understood, information about the characteristics of the laser pulse can be obtained. For instance, in atoms, where an accurate description of the electrons can be obtained, the carrier-envelope phase difference may be extracted in this way [8–10]. For molecules, the extra nuclear degrees of freedom may be used to control the process of interest. As an example, the ability to orient molecules [11] with respect to an external axis may be used to enhance the high-order harmonic yield [12–15]. Solving the dynamics of the molecule in the strong field is, however, much more difficult than the atom due to the extra degrees of freedom. In fact, not even the simplest case of H_2^+ interacting with strong IR fields has been solved in full six-dimensional calculations. Fortunately, the interesting prospect of ever shorter pulse durations introduces a simplification in the description: the time scales of rotation and vibration are often much longer than the actual applied pulses themselves, and therefore some of these degrees of freedom may be treated as frozen during the interaction with the field. In the present work, we describe how frozen degrees of freedom affect the outcome of an experiment in a nontrivial manner. We show that the influence of the dynamics and the formulation of the theory of measurement depend very much on the process considered: we obtain completely different behavior for above-threshold ionization (ATI) and high-order harmonic generation (HHG) with respect to the coherence in the signal from rotational degrees of freedom. The discussion is exemplified using realistic alignment and orientation schemes.

We consider HHG and ATI in molecules interacting with a short strong laser pulse. We use the single-particle density operator $\hat{\rho}(t_0)$ for calculations [16]. At time $t=t_0$ prior to any pulse, the molecule is in a time-independent thermal state at temperature T. By definition, $\hat{\rho}(t_0)=\exp(-\hat{H}/k_BT)/Z$, with partition function $Z=\mathrm{Tr}[\exp(-\hat{H}/k_BT)]$, $\hat{H}$ is the field-free molecular Hamiltonian, and k_B is Boltzmann's constant. The initial state is resolved on energy eigenstates $|\boldsymbol{\alpha}\rangle$ with energy $E_{\boldsymbol{\alpha}}$. We concentrate on diatomics where, prior to the applied pulses, only the electronic and vibrational ground states are populated. Consequently, the energy eigenstate is characterized by the angular momentum quantum number, J, and its projection on a space fixed axis, M, i.e., $\boldsymbol{\alpha}=(J,M)$. The discussion is straightforwardly generalized to more complicated cases and the conclusions remain unaffected. There is no decay on the time scales we are considering so propagation is described by a unitary operator $\hat{U}(t)$, $\hat{U}(t)|\boldsymbol{\alpha}\rangle=|\Psi_{\boldsymbol{\alpha}}(t)\rangle$, $\hat{\rho}(t)=\hat{U}(t)\hat{\rho}(t_0)\hat{U}^{\dagger}(t)=\Sigma_{\boldsymbol{\alpha}}P_{\boldsymbol{\alpha}}|\Psi_{\boldsymbol{\alpha}}(t)\rangle\langle\Psi_{\boldsymbol{\alpha}}(t)|$, with the Boltzmann weight $P_{\boldsymbol{\alpha}}=\exp(-E_{\boldsymbol{\alpha}}/k_BT)/Z$. The evolution due to $\hat{U}(t)$ can contain both alignment pulses and a subsequent short probe pulse producing ATI and HHG.

We separate out the relatively slow rotational movement of the nuclei $\Psi_{JM}(\boldsymbol{r}_e,R,\Omega,t)\approx\psi(\boldsymbol{r}_e,R,t;\Omega)\phi_{JM}(\Omega,t)$, with R the internuclear distance and $\Omega=(\theta,\phi)$ the spherical polar and azimuthal angles. The variables that enter parametrically in the wave function are set after the semicolon. If we consider the response to a femtosecond probe pulse centered at t_p, the rotational degrees of freedom can be considered frozen during the pulse and the full wave function is approximated by

$$\Psi_{JM}(\boldsymbol{r}_e,R,\Omega,t)\approx\psi(\boldsymbol{r}_e,R,t;\Omega,t_p)\phi_{JM}(\Omega,t_p). \tag{1}$$

In the case of a prealigning or orienting pump pulse between t_0 and t_p, $\phi_{JM}(\Omega,t_p)$ is the rotational wave packet evolving from $Y_{JM}(\Omega)$ at time t_0. If no pump pulse is used $\phi_{JM}(\Omega,t_p)=Y_{JM}(\Omega)$.

Treating HHG first, the complex amplitude for the emission of harmonics polarized along the unit vector $\boldsymbol{e}$ with frequency ω, is obtained from the Fourier transform of the dipole acceleration

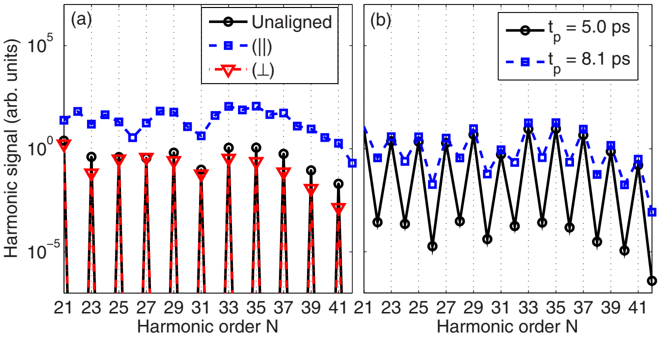

FIG. 1. (Color online) Harmonic generation from CO by (5) illustrating the dramatic effects of molecular orientation. The signal is polarized along the linearly polarized driving laser of wavelength 800 nm and intensity 2×10^{14} W/cm^2. (a) HHG yield for (i) an isotropic, unaligned ensemble, (ii) perfect orientation along the driving laser polarization (∥), and (iii) perfect orientation perpendicular to the driving laser polarization (⊥). (b) HHG yield from CO after field-free orientation by a half-cycle pump pulse. The delay of the probe pulse with respect to the orienting pulse is denoted by t_p.

$$A_{\boldsymbol{e}}(\omega) = \boldsymbol{e}\cdot\int dt e^{-i\omega t}\frac{d^2}{dt^2}\langle\hat{\boldsymbol{d}}\rangle(t), \tag{2}$$

with $\langle\hat{\boldsymbol{d}}\rangle(t)=\mathrm{Tr}[\hat{\rho}(t)\hat{\boldsymbol{d}}]=\Sigma_{\boldsymbol{\alpha}}P_{\boldsymbol{\alpha}}\langle\Psi_{\boldsymbol{\alpha}}(t)|\hat{\boldsymbol{d}}|\Psi_{\boldsymbol{\alpha}}(t)\rangle$ the expectation value of the dipole operator $\hat{\boldsymbol{d}}$ of the molecule. The corresponding power density reads [17,18] as follows:

$$S_{\boldsymbol{e}}(\omega)\propto|A_{\boldsymbol{e}}(\omega)|^2. \tag{3}$$

We note that one can observe interferences in the intensity $S(\omega)$ from incoherent members of the ensemble, i.e., members belonging to different $\boldsymbol{\alpha}$. This effect of intensity interferences stemming from adding electric fields is known as polarization beats to distinguish it from coherent quantum beats.

We insert the wave functions (1) into the expression for $\langle\hat{\boldsymbol{d}}\rangle(t)$ and obtain $\langle\hat{\boldsymbol{d}}\rangle(t)=\int d\Omega G(\Omega,t_p)\langle\hat{\boldsymbol{d}}\rangle^{e,\mathrm{vib}}(t;t_p,\Omega)$, with the vibronic dipole $\langle\hat{\boldsymbol{d}}\rangle^{e,\mathrm{vib}}(t;t_p,\Omega)=\langle\psi(t;t_p,\Omega)|\hat{\boldsymbol{d}}_e|\psi(t;t_p,\Omega)\rangle$ and

$$G(\Omega,t_p)=\sum_{JM}P_J|\phi_{JM}(\Omega,t_p)|^2, \tag{4}$$

the angular distribution at time t_p. The corresponding spectrum is obtained from (2) and (3)

$$S(\omega,t_p)\propto\left|\int d\Omega G(\Omega,t_p)A_{\boldsymbol{e}}^{e,\mathrm{vib}}(\omega,\Omega,t_p)\right|^2, \tag{5}$$

with $A_{\boldsymbol{e}}^{e,\mathrm{vib}}(\omega,\Omega,t_p)$ the complex amplitude for generation of harmonics at frequency ω and polarization $\boldsymbol{e}$ from the electronic dipole $\langle\hat{\boldsymbol{d}}\rangle^{e,\mathrm{vib}}(t;t_p,\Omega)$ in a molecule fixed at Ω. If no alignment pulses are used, $G(\Omega,t_p)$ is isotropic. This follows from $G(\Omega,t_p)=\Sigma_J P_J\Sigma_M|Y_{JM}(\Omega)|^2=\Sigma_J P_J(2J+1)/(4\pi)$ which is indeed independent of angles. In this case, the spectrum arises from the coherent summation of amplitude contributions from different orientations, $A_{\boldsymbol{e}}^{e,\mathrm{vib}}(\omega,\Omega,t_p)$, independent on the temperature of the sample. In general, the signals always contain optical coherences, except in the case $G(\Omega,t_p)=\delta(\Omega-\Omega')$. Apart from being physically well justified and displaying the effects of the frozen molecular degrees of freedom, the relevance of (5) is that the numerical propagation during the ultrashort pulse is immensely more manageable when the dimensionality is reduced. For molecules with vibrational frequencies much smaller than the inverse duration of the applied laser pulse, the vibrational coordinates can also be treated as fixed, and one can separate out the vibrational part of the vibronic wave function in (5) as well. The very different time scales allow the pulse to consist of, say, 10 cycles and therefore we can treat the field as monochromatic in the simple calculations illustrating the effects. For CO with frozen rotations, Fig. 1 shows the results of simulations of the emitted high-order harmonics of the same polarization as the linearly polarized driving laser of wavelength 800 nm probe field with peak intensity 2×10^{14} W/cm^2. We use a quantum mechanical three-step model to calculate the harmonic signal [19]. Figure 1(a) shows three cases corresponding to (i) uniform orientational distribution, (ii) perfect parallel orientation, i.e., the permanent molecular dipole, pointing from O to the less electronegative C, is directed along the polarization vector of the probe pulse, and (iii) perfect perpendicular orientation. Figure 1 shows that the HHG signal depends critically on the direction of the orientation. There is no dependence of the azimuthal angle in any of the cases, so we only consider the polar part of the solid angle. We first discuss (ii) and (iii) and return to (i) at the end of this section. The occurrence (ii) and absence (iii) of even harmonics in the signal may be understood by recalling that emission of harmonic of order N comprises $N+1$ dipole transitions (N absorptions of a laser photon, and the emission of a single high-order harmonic photon). In case (ii), only the component $\hat{\parallel}$ of the dipole operator parallel to the internuclear axis is active and this component has a $\Delta\Lambda=0$ selection rule, with Λ the absolute value of the projection of the electronic orbital angular momentum on the internuclear axis. Initially the molecule is in its Σ ground state and because of $\Delta\Lambda=0$ it stays in the manifold of Σ states. The Σ state, from which the final recombination step occurs, is hence accessible by the absorption of both an even and odd number of photons and, consequently, both even or odd harmonics are produced. Turning to (iii), only the component $\hat{\perp}$ of the dipole operator perpendicular to the internuclear axis is active and this component has a $\Delta\Lambda=\pm1$ selection rule. Consequently, only odd harmonics are observed since the Π state, from which the recombination occurs, can only be reached by the absorption of an odd number of photons. In the unaligned case (i), the situation is analyzed by considering the transition operator $\hat{O}_N=\Pi_{i=1}^{N+1}(\hat{\parallel}_i\cos\theta+\hat{\perp}_i\sin\theta)$ corresponding to emission of a harmonic of order N for a molecule with the permanent dipole oriented at an angle θ with respect to the polarization vector of the probe laser field. In the limits of parallel ($\theta=0°$) and perpendicular ($\theta=90°$) orientation we retrieve the results discussed above. In general the operator $\hat{O}_N$ contains even and odd powers of cosines and sines. In the unaligned case $G(180°-\theta,t_p)=G(\theta,t_p)$, and we see from (5) that only combinations of the cosines and sines yielding an even function on $[0,180°]$ will survive, i.e., the terms containing an even number of the $\hat{\parallel}_i$ operator. From the selection rules it is, however, clear that the total number of Λ changing transition must be an even number and thus the total number of dipole transitions is even, explaining why only odd harmonics are emitted in the unaligned case.

In order to simulate a more realistic orientational distribution, we present in Fig. 1(b) the prediction of the harmonic signal from an ensemble of partially oriented CO molecules. To obtain orientation, a half-cycle pulse (HCP) with amplitude 870 kV/cm and a duration of 0.5 ps [full width at half-maximum (FWHM)] is followed 4.14 ps later by a linearly polarized laser pulse of 0.5 ps duration and a peak intensity of 5×10^{12} W/cm^2. In order to model the orientation we solve the time-dependent Schrödinger equation for the rotational degrees of freedom with rotational constant $B=57.9$ GHz, dipole moment $\mu=0.112$ D, and polarizability volume components $\alpha_{\parallel}=1.925$ Å^3 and $\alpha_{\perp}=1.420$ Å^3 [20]. The initial rotational temperature is 5 K. The probe field which generates high-order harmonics is the same as in Fig. 1(a). We plot the harmonic signal at two different delays with respect to the peak of the HCP. The time delay $t_p=5$ ps is chosen to illustrate the case with an almost symmetric orientational distribution: $G(180°-\theta,5\text{ ps})\simeq G(\theta,5\text{ ps})$, and in this case the even harmonics are suppressed as expected from arguments similar to the ones used in the discussion of the unaligned case in Fig. 1(a). At longer delays the molecules have time to orient, obtaining a maximum after 8.1 ps with $\langle\cos\theta\rangle=-0.11$. At this time delay the CO dipoles tend to be pointing opposite to the polarization vector of the HCP, and this asymmetric distribution allows for even and odd harmonics of comparable strength.

We now turn to a discussion of ATI. The fundamental quantity is the probability $W(\boldsymbol{k})$ for measuring the momentum $\boldsymbol{k}$ of the outgoing electron. The associated measurement operator is $\hat{\mathcal{P}}_{\boldsymbol{k}}=|\psi_{\boldsymbol{k}}^-\rangle\langle\psi_{\boldsymbol{k}}^-|\otimes\hat{I}_R$ which projects on an electron scattering state $|\psi_{\boldsymbol{k}}^-\rangle$ with asymptotic momentum $\boldsymbol{k}$ and leaves the nuclei unaffected $(\hat{I}_R)$. Accordingly, $W(\boldsymbol{k})=\langle\hat{\mathcal{P}}_{\boldsymbol{k}}\rangle=\mathrm{Tr}[\hat{\rho}(t)\hat{\mathcal{P}}_{\boldsymbol{k}}]$ where $\hat{\rho}(t)$ is the density matrix of the system. We evaluate the trace in the position-eigenstate basis and obtain $W(\boldsymbol{k})=\int d\boldsymbol{r}_e\int d\boldsymbol{R}\langle\boldsymbol{r}_e,\boldsymbol{R}|\hat{\rho}(t)\hat{\mathcal{P}}_{\boldsymbol{k}}|\boldsymbol{r}_e,\boldsymbol{R}\rangle=\Sigma_\alpha P_\alpha\int d\boldsymbol{R}|\int d\boldsymbol{r}_e\psi_{\boldsymbol{k}}^{-\star}(\boldsymbol{r}_e)\Psi_\alpha(\boldsymbol{r}_e,\boldsymbol{R},t)|^2$. Introducing the wave functions (1), we obtain

$$W(\boldsymbol{k},t_p)=\int d\Omega G(\Omega,t_p)\int dRR^2|A(\boldsymbol{k};\boldsymbol{R},t_p)|^2, \qquad (6)$$

with $G(\Omega,t_p)$ defined in (4) and the complex amplitude $A(\boldsymbol{k};\boldsymbol{R},t_p)=\int d\boldsymbol{r}_e\psi_{\boldsymbol{k}}^{-\star}(\boldsymbol{r}_e)\psi(\boldsymbol{r}_e,R,t;\Omega,t_p)$ describing the transition for frozen rotations at time t_p. The time t may be any time after the ionizing pulse. In contrast to the HHG signal (5) which is optically coherent in nuclear orientations, the signal for ATI is obtained as an incoherent summation of contributions from different molecular orientations. As was the case for the HHG process, the calculations involved in the evaluation of (6) are vastly simplified if the rotational and/or the vibrational degrees of motion are frozen during the femtosecond pulse. Figure 2 shows angular distributions of the outgoing electron for N_2 and O_2 for isotropic and field-free aligned samples. We obtain the angular distributions by integrating (6) over the magnitude of the momentum. In the present calculation, we approximate the transition amplitude in (6) by the molecular strong-field approximation amplitude [21]. The degrees of alignment are determined by the procedure described in [22], and we use the following parallel (perpendicular) polarizability volume of N_2, 2.38 Å^3 (1.45 Å^3) and of O_2, 2.3 Å^3 (1.1 Å^3). The linearly polarized aligning pulse has peak intensity 4×10^{13} W/cm^2 and duration 59 fs (FWHM). The initial rotational temperature is 11 K. For the relatively low initial rotational temperature assumed here, the maximum alignment occurs at the one-quarter revival period (2.1 ps after the pump pulse for N_2 and 2.9 ps delay for O_2). The corresponding values of $\langle\cos^2\theta\rangle$ are 0.71 (N_2) and 0.74 (O_2). We present results both for alignment preferentially along the polarization axis of the probe laser and for alignment along an axis perpendicular to the probe polarization. For N_2, the only effect of making $G(\Omega,t_p)$ anisotropic is a change in the overall scaling. This is due to the Σ_g symmetry of the initial orbital and is in accordance with the predictions of tunneling theory which favors electron ejection along the polarization direction [23]. In the case of O_2, we find a more pronounced effect of the orienta-

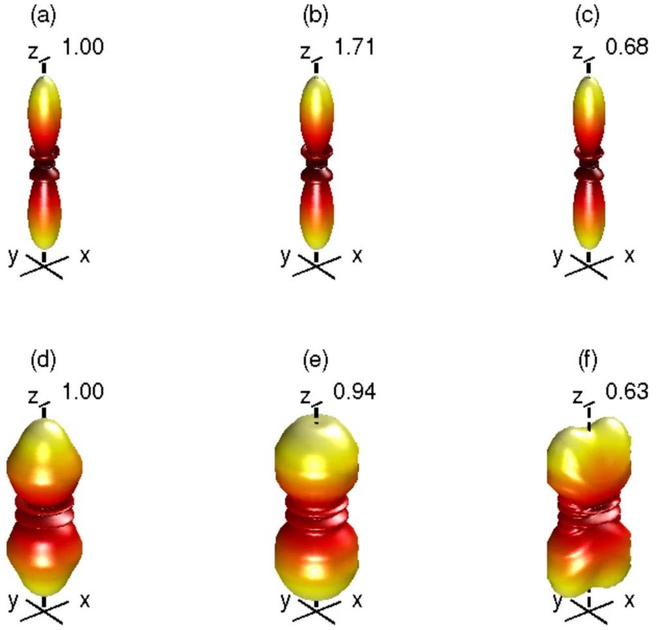

FIG. 2. (Color online) Angular differential ionization rates. We use an 800 nm probe laser polarized along the z axis for N_2 (a)–(c) at 2×10^{14} W/cm^2 and O_2 (d)–(f) at 1.2×10^{14} W/cm^2. (a) N_2 isotropic, unaligned ensemble. (b) N_2, the degree of alignment peaks along the z axis. (c) N_2, the degree of alignment peaks along the x axis. (d) O_2 isotropic, unaligned ensemble. (e) O_2, the degree of alignment peaks along the z axis. (f) O_2, the degree of alignment peaks along the x axis. The numbers adjacent to the z axis indicate the scale with respect to the randomly aligned cases (a) and (d). The plots present the predictions of (6) for experimentally realizable degrees of alignment.

tion. The change in angular pattern reflects the symmetry of the initial Π_g orbital which has zero amplitude along and perpendicular to the molecular axis: this nodal structure forbids the electron escaping along the vertical polarization axis when perfectly aligned, hence the change from (d) to (e) and (f).

In conclusion, we have developed the theory of how to deal with frozen nuclear degrees of freedom in HHG and ATI. The frozen coordinates affect the motion in a nontrivial way and coherence issues depend on the degree of orientation. Physically, the phase coherence in HHG with respect to different orientations may be understood by the superposition principle for the electric field generated by an ensemble of oscillators with different orientations. The reason for absence of coherence in the ATI signal from different orientations is that an experimentalist has the option, in principle, of determining the orientation at the instant of ionization by, e.g., detecting in coincidence a dissociating pair of nuclei. The present work forms the theoretical basis for future work on molecules interacting with strong short pulses.

This work is supported by the Danish Research Agency (Grant. No. 2117-05-0081).

---

[1] A. Baltuška *et al.*, Nature (London) **421**, 611 (2003).

[2] J. Itatani, J. Levesque, D. Zeidler, H. Niikura, H. Pépin, J. C. Kieffer, P. B. Corkum, and D. M. Villeneuve, Nature (London) **432**, 867 (2004).

[3] H. Niikura, F. Légaré, R. Hasbani, A. D. Bandrauk, M. Y. Ivanov, D. M. Villeneuve, and P. B. Corkum, Nature (London) **417**, 917 (2002).

[4] H. Niikura, F. Légaré, R. Hasbani, M. Y. Ivanov, D. M. Villeneuve, and P. B. Corkum, Nature (London) **421**, 826 (2003).

[5] A. S. Alnaser *et al.*, Phys. Rev. Lett. **93**, 183202 (2004).

[6] A. S. Alnaser, T. Osipov, E. P. Benis, A. Wech, B. Shan, C. L. Cocke, X. M. Tong, and C. D. Lin, Phys. Rev. Lett. **91**, 163002 (2003).

[7] S. Baker, J. S. Robinson, C. A. Haworth, H. Teng, R. A. Smith, C. C. Chirila, M. Lein, J. W. G. Tisch, and J. P. Marangos, Science **312**, 424 (2006).

[8] G. G. Paulus, F. Lindner, H. Walther, A. Baltuška, E. Goulielmakis, M. Lezius, and F. Krausz, Phys. Rev. Lett. **91**, 253004 (2003).

[9] C. A. Haworth, L. E. Chipperfield, J. S. Robinson, P. L. Knight, J. P. Marangos, and J. W. G. Tisch, Nat. Phys. **3**, 52 (2007).

[10] Christian Per Juul Martiny and L. B. Madsen, Phys. Rev. Lett. **97**, 093001 (2006).

[11] H. Stapelfeldt and T. Seideman, Rev. Mod. Phys. **75**, 543 (2003).

[12] N. Hay, R. Velotta, M. Lein, R. de Nalda, E. Heesel, M. Castillejo, and J. P. Marangos, Phys. Rev. A **65**, 053805 (2002).

[13] J. Itatani, D. Zeidler, J. Levesque, M. Spanner, D. M. Villeneuve, and P. B. Corkum, Phys. Rev. Lett. **94**, 123902 (2005).

[14] T. Kanai, S. Minemoto, and H. Sakai, Nature (London) **435**, 470 (2005).

[15] M. Lein, R. de Nalda, E. Heesel, N. Hay, E. Springate, R. Velotta, M. Castillejo, P. L. Knight, and J. P. Marangos, J. Mod. Opt. **52**, 465 (2005).

[16] For HHG, phase matching is an important issue, but experimental conditions can be obtained where the use of the single-particle approach is valid, J. Levesque, D. Zeidler, J. P. Marangos, P. B. Corkum, and D. M. Villeneuve, Phys. Rev. Lett. **98**, 183903 (2007).

[17] B. Sundaram and P. W. Milonni, Phys. Rev. A **41**, 6571 (1990).

[18] K. Burnett, V. C. Reed, J. Cooper, and P. L. Knight, Phys. Rev. A **45**, 3347 (1992).

[19] C. B. Madsen and L. B. Madsen, Phys. Rev. A **74**, 023403 (2006).

[20] Y. Y. Liao, Y. N. Chen, and D. S. Chuu, Phys. Rev. B **70**, 233410 (2004).

[21] T. K. Kjeldsen and L. B. Madsen, J. Phys. B **37**, 2033 (2004).

[22] J. Ortigoso, M. Rodríguez, M. Gupta, and B. Friedrich, J. Chem. Phys. **110**, 3870 (1999).

[23] T. K. Kjeldsen and L. B. Madsen, Phys. Rev. A **74**, 023407 (2006).